Importance of Force Linkage in Mechanochemistry of Adhesion Receptors[†]

Nathan S. Astrof, Azucena Salas,[‡] Motomu Shimaoka, JianFeng Chen, and Timothy A. Springer*

The CBR Institute for Biomedical Research, Department of Anesthesia and Department of Pathology, Harvard Medical School, Boston, Massachusetts 02115

Received August 2, 2006; Revised Manuscript Received September 26, 2006

ABSTRACT: The α subunit-inserted (I) domain of integrin $\alpha_L\beta_2$ [lymphocyte function-associated antigen-1 (LFA-1)] binds to intercellular adhesion molecule-1 (ICAM-1). The C- and N-termini of the α I domain are near one another on the "lower" face, opposite the metal ion-dependent adhesion site (MIDAS) on the "upper face". In conversion to the open α I domain conformation, a 7 Å downward, axial displacement of C-terminal helix α7 is allosterically linked to rearrangement of the MIDAS into its high-affinity conformation. Here, we test the hypothesis that when an applied force is appropriately linked to conformational change, the conformational change can stabilize adhesive interactions that resist the applied force. Integrin α I domains were anchored to the cell surface through their C- or N-termini using type I or II transmembrane domains, respectively. C-terminal but not N-terminal anchorage robustly supported cell rolling on ICAM-1 substrates in shear flow. In contrast, when the α_L I domain was mutationally stabilized in the open conformation with a disulfide bond, it mediated comparable levels of firm adhesion with type I and type II membrane anchors. To exclude other effects as the source of differential adhesion, these results were replicated using α I domains conjugated through the N- or C-terminus to polystyrene microspheres. Our results demonstrate a mechanical feedback system for regulating the strength of an adhesive bond. A review of crystal structures of integrin α and β subunit I domains and selectins in high- and low-affinity conformations demonstrates a common mechanochemical design in which biologically applied tensile force stabilizes the more extended, high-affinity conformation.

The ability of leukocytes to engage in a rolling adhesive interaction on endothelium is important as the first step in surveying endothelium for signals that trigger emigration. Rolling of leukocytes is driven by the hydrodynamic force of the bloodstream acting on an adherent cell and involves jerky stepwise movements of the cell that reflect receptor−ligand bond dissociation events. Rolling can be reproduced *in vitro* using leukocytes or transfectants in parallel wall flow chambers to which purified adhesion ligands are absorbed. Poised between firm adhesion and mechanically induced detachment, stable rolling requires bond dissociation under mechanical stress at the upstream edge of a cell to be balanced by the re-formation of bonds downstream in the adhesion zone between cell and substrate (*1*). Significantly, physiological rolling interactions are highly stable, both *in vivo* and *in vitro*, to alterations in surface ligand density and to the hydrodynamic force acting on the cell, which is proportional to the wall shear stress.

Why rolling is so stable is imperfectly understood, although both cellular and molecular features contribute to the stability of rolling (*1*−*7*). One important factor as shear increases is the increase in the number of receptor−ligand bonds between the cell and the substrate, which compensates for faster bond dissociation (*1*). Another factor is the mechanical stability of individual bonds, i.e., a low coefficient of increase in the rate of bond dissociation with an increase in force (*2*−*6*, *8*). Molecular specializations may be important, since among adhesion molecules, all selectin−ligand interactions and a subset of integrin−ligand interactions support rolling, whereas IgSF−IgSF and cadherin−cadherin interactions robustly support firm adhesion but not rolling adhesion (*9*). Only a small subset of antibody−antigen pairs support rolling, and those that do exhibit limited stability (*10*). Rapid bond association and dissociation kinetics appear to be required but are not sufficient to support rolling, as shown with interacting IgSF adhesion molecules CD2 and LFA-3, which have kinetics in the appropriate range (*11*, *12*) but fail to support rolling (*13*). Given these considerations, it is intriguing that the classes of adhesion molecules that support rolling, selectins and integrins, undergo inter- and intradomain allosteric rearrangements that are linked to changes in affinity for ligand (*14*−*19*).

In this study, we examine force as an allosteric effector of an integrin domain that supports rolling. Previously, it has been shown that the isolated integrin LFA-1 α I domain

[†] Supported by National Institutes of Health Grant HL48675.

* To whom correspondence should be addressed. E-mail: springeroffice@cbr.med.harvard.edu. Phone: (617) 278-3200. Fax: (617) 278-3232.

[‡] Current address: Instituto de Investigaciones Biomedicas de Barcelona-CISC, Rosello 161, 7a planta, 08036 Barcelona, Spain.

[1] Abbreviations: LFA-1, lymphocyte function-associated antigen-1; ICAM-1, intercellular adhesion molecule-1; MIDAS, metal ion-dependent adhesion site; IgSF, immunoglobulin supergene family; LFA-3, lymphocyte function-associated antigen-3; IPDGFR, I domain linked to platelet-derived growth factor receptor transmembrane domain; PCR, polymerase chain reaction; PBS, phosphate-buffered saline; HBSS, Hank's balanced salt solution; HSA, human serum albumin; EDTA, ethylenediaminetetraacetate; TM, transmembrane; EGF, epidermal growth factor; FITC, fluorescein isothiocyanate; IgG, immunoglobulin G.

10.1021/bi061566o CCC: $33.50
Published on Web 11/22/2006

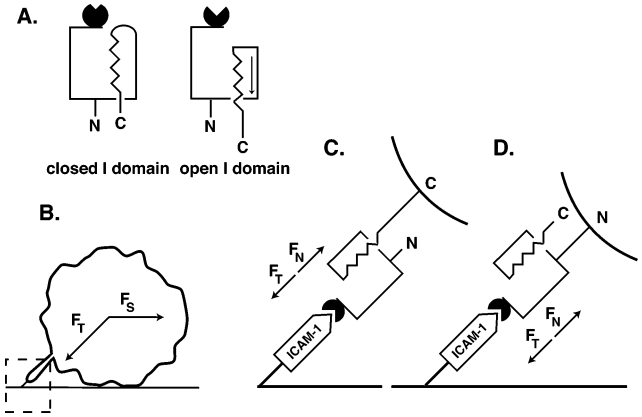

FIGURE 1: I domain allostery and force. (A) Schematic representation of the I domain. The transition of the MIDAS from the closed to open conformation is linked to an axial, C-terminal shift of the C-terminal α helix (arrow). (B) Schematic of a cell adhering to a substrate in shear flow, with hydrodynamic force on the cell (F_S) and force on the tether (F_T). (C and D) The boxed region in panel B is magnified to show the tether to the substrate through the I domain−ICAM-1 interaction. ICAM-1 is shown linked to the substrate (straight line, bottom), and the I domain is shown linked to the cell surface (curved line, top right). The tether force (F_T) is balanced by an equal but oppositely disposed normal force (F_N).

can mediate shear-resistant cell rolling interactions on intercellular adhesion molecule-1-coated surfaces in hydrodynamic flow when fused through its C-terminus to a type I transmembrane domain (*20*). The ligand ICAM-1[1] is a cell-surface IgSF molecule. The LFA-1 α I domain adopts an α/β fold with seven α helices surrounding a six-stranded β sheet. A Mg(II) ion in a metal ion-dependent adhesion site (MIDAS) on the upper face of the I domain coordinates a Glu residue in ligands such as ICAM-1. Amino acid residues that contact I domain ligands surround the MIDAS on the upper face, while the N- and C-terminal connections to the integrin β propeller are located on the opposite, lower face. In the activated (open, high-affinity) conformation of the α I domain, C-terminal helix α7 is displaced downward with respect to the position found in the basal (closed, low-affinity) conformation (Figure 1A). The position of helix α7 allosterically regulates the conformation of loops bearing metal coordinating and ICAM-1 binding residues and hence affinity for the ligand (*18*).

The wild-type, isolated α I domain exists predominantly in the closed, low-affinity conformation; however, it must transition to the open, high-affinity conformation to support rolling, since rolling is inhibited by small molecule antagonists that bind to and stabilize the closed conformation (*21*). Binding to ICAM-1 stabilizes the open conformation, as shown in NMR experiments in which high concentrations of ICAM-1 and wild-type α I domain drive the equilibrium toward complex formation (*22*). While the affinity of the wild-type, isolated α I domain for ICAM-1 is weak ($K_d \sim 1$ mM), the affinity of a mutant α I domain with the C-terminal helix locked in the downward (open) conformation is enhanced approximately 10000-fold (*23*). Targeted molecular dynamics simulations showed that force applied to the C-terminal helix of the wild-type α I domain could drive the transition from the closed (low-affinity) to open (high-affinity) state and that the extent of the conformational transition was related to the force that was applied (*24*).

Here, we test the hypothesis that rolling can be stabilized if force is applied to a receptor−ligand complex through a linkage that enables the applied force to favor a conformational state that has a higher affinity for the ligand (Figure 1A,B). We have previously suggested that stable rolling by the integrin α I domain is critically dependent upon the linkage of the I domain to the cell through the C-terminus (*21*). We explicitly test this hypothesis by comparing α I domains that are anchored to cells or beads through either their N- or C-termini. Furthermore, a structural analysis of other adhesion receptors shows that they have a mechanochemistry such that physiologic tensile force exerted on the receptor−ligand complex favors the more extended, high-affinity conformation.

EXPERIMENTAL PROCEDURES

Reagents. Pfu polymerase and deoxynucleotide mix were from Stratagene (Ceder Creek, TX). Restriction enzymes, alkaline phosphatase, and T4 DNA ligase were from New England Biolabs (Beverly, MA). Vectors pcDNA3.1(+)-hygro and pcDNA3.1(+)-puro were from Invitrogen (Carlsbad, CA). Biotin ligase (BirA) was from Avidity (Bolder, CO), and streptavidin-coated microspheres were from Bangs Labs (Fishers, IN). ICAM-1-Fcγ was from R&D Systems (Minneapolis, MN), and human serum albumin (HSA) was from Sigma (St. Louis, MO). Antibodies X63 and TS1/11, used as culture supernatants, have been described previously (*25*). Purified mouse IgG1 was from BD Biosciences (San Jose, CA), and MHM24 (*26*) was from Dako Cytomation (Carpenteria, CA).

cDNAs, Cell Lines, and Proteins. K562 cells stably transfected with the type I α_L I domain (both the wild type and the K287C/K294C mutant) fused to the platelet-derived growth factor receptor transmembrane domain (IPDGFR) have been described previously (*27*). The type II α_L I domain was fused to the Us9 (Δ46−55) transmembrane domain (*28*, *29*) via a flexible linker in three steps. The native Us9 protein is present in two forms, differing in the position of the N-terminal methionine. Our construct begins at the second (internal) start position. Each segment of the synthetic gene was prepared by PCR; unique restriction sites (underlined) were added to facilitate assembly. Sequences were confirmed by DNA sequencing. The following set of PCR primers was used: Primer_1^{forward}, TAGAAGCTTATGGACACGTTCGACCCCAGCGCC; Primer_1^{reverse}, TTAAGGATCCACCTGAACCCACGTGCCGGGATGATGCC; Primer_2^{forward}, TATAGGATCCGCTTCCTCCGGAGGTGGTTCAGGCAACGTAG; Primer_2^{reverse}, ATTTCTCGAGTTAATAGATCTTCTTCTTCTGCAGCTCAG; Primer_3^{forward}, ATAAAGGATCCGCTGGCGCCTCCTCCAGCGCTGTCGACGAACAAAAACTCATC; and Primer_3^{reverse}, AATAATCCGGAACCACCAGAAGCAGAGAGCCAGCGCCGGTACCCACGATGACCTCCTGGGTGTC.

The Us9 (Δ46−55) gene was amplified from pAB35 (kindly provided by L. W. Enquist, Department of Microbiology, Princeton University, Princeton, NJ) using primer set 1. The vector pcDNA3.1(+)-hygro and PCR product were digested with HindIII and BamHI and ligated to give plasmid pCUS9. Using primer set 2, linker residues and residues G128−Y307 of the α_L I domain were amplified from a previously described (*30*) vector denoted pNBirI that

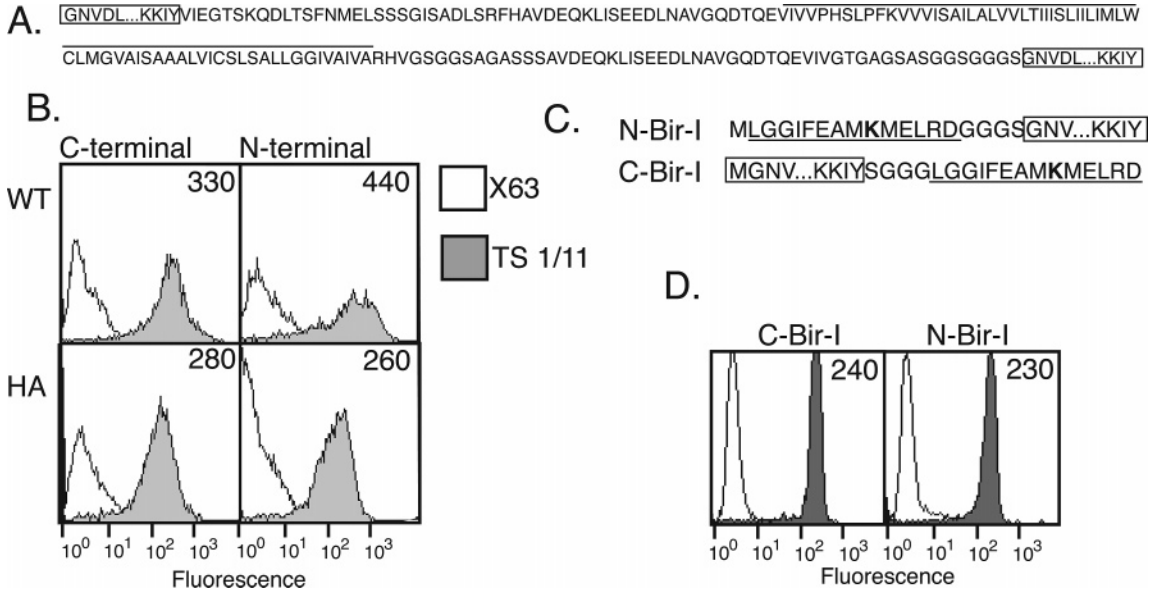

FIGURE 2: N- and C-terminally anchored I domains. (A) Sequences for type I (top) and type II (bottom) TM domain-anchored I domains. I domain sequence is boxed, and the first five (GNVDL) and last four (KKIY) residues are shown for reference. The TM domains are overlined. The linker sequence is between the boxed and overlined sequence. (B) Flow cytometry of type I and type II TM domain I domains. Cells were stained with (gray) a 1:10 dilution of TS1/11 culture supernatant or (white) control X63 myeloma supernatant, detected by FITC-labeled goat anti-mouse IgG (2 μg/mL). (C) Sequences for biotinylated, soluble I domains. The I domain sequence is boxed, and beginning and end residues are shown for reference. The Bir A tag is underlined, and the biotinylated lysine is bold. (D) Streptavidin-coated microspheres linked to biotinylated I domains, stained with a 1:5 dilution of TS1/11 culture supernatant (gray) or X63 (white), detected with 2 μg/mL FITC-labeled goat anti-mouse IgG.

encodes the sequence shown in Figure 2C. The PCR product and pCUS9 were digested with BamHI and XhoI and ligated to give the pCALIUS9_short vector, and then the HindIII and XhoI fragment was subcloned into pcDNA3.1(+)-puro. Primer set 3 was used to amplify a linker segment from pIPDGFR (*27*). The PCR product and the HindIII and XhoI fragment subcloned above into pcDNA3.1(+)-puro were digested with BamHI and BspEI and ligated to give the pALIUS9-puro vector. The HindIII and XhoI fragment was then subcloned into pcDNA3.1(+)-hygro to give pALIUS9-hygro. A construct expressing the K287C/K294C (high-affinity) mutant I domain was prepared in an analogous fashion except the template for PCR step 2 was the vector encoding the N-terminal fusion of the Bir tag with the mutant I domain.

K562 cells (20×10^6) were transfected with 20 μg of DNA at 250 mV and 960 μF by electroporation. Transfectants were selected in medium containing 100 μg/mL hygromycin. After 2 weeks, cells were stained at 4 °C for 30 min with TS1/11 antibody (1:20 dilution) and the nonbinding X63 myeloma (1:20 dilution) as a negative control, washed and stained with PE-conjugated goat anti-mouse IgG at 4 °C for 30 min, and washed again, and the brightest 1% of the cells were selected by fluorescence-activated cell sorting. After further growth, the brightest 0.1% of the cells were sorted one cell per well into 96-well plates. Clones expressing high levels of wild-type and high-affinity type II I domains were then selected. All cells were maintained in RPMI 1640 medium supplemented with 10% fetal calf serum, 2 mM glutamine, 500 units/mL penicillin, 500 μg/mL streptomycin, and 100 μg/mL hygromycin.

Type I and Type II Biotinylated Soluble I Domains. The expression, refolding, purification, and biotinylation with BirA ligase of recombinant soluble I domains fused to the BirA consensus sequence were exactly as previously described for the N-terminally tagged I domain (*30*). The final step was S75 gel permeation chromatography, which showed that the material was monomeric. The C-terminally tagged I domain construct was made as described for the N-terminally tagged construct, with an initiation methionine, I domain residues G128−Y307, the linker Ser-Gly-Gly-Gly, and the BirA enzyme recognition tag (LGGIFEAMK-MELRD) (Figure 2C). The biotinylated soluble I domain [5 μg/mL in PBS (pH 7.4) and 1% BSA] was attached to 9.95 μm streptavidin microspheres according to the manufacturer's instructions, washed in the same buffer, and used within 1 h.

Preparation of Cells. Cells were washed twice in HBSS without Ca(II) or Mg(II), once in HBSS and 5 mM EDTA, and twice in HBSS without Ca(II) or Mg(II). Cells were suspended at a final concentration of 5×10^6 cells/mL in HBSS without Ca(II) or Mg(II) and kept at room temperature prior to each experiment.

Accumulation in Shear Flow and Rolling Velocity. A polystyrene plate was coated with a 20 μL spot of ICAM-1-Fcγ (10 μg/mL) in PBS buffer (pH 9.0) with 10 mM sodium bicarbonate at 37 °C for 1 h. The plate was washed with a small amount of the same buffer and blocked with 2% HSA in the same buffer at 37 °C for 1 h.

ICAM-1 substrates were assembled as the lower wall in a parallel plate flow chamber and mounted on the stage of an inverted phase-contrast microscope. A syringe pump with a 3 mL plastic syringe was used to generate the desired shear stress conditions. Cells were resuspended in HBSS buffer, 1 mM Ca(II), and 1 mM Mg(II) except for control experiments as described. Cells (0.5 mL at a density of 5×10^5 cells/mL) were perfused into a parallel plate flow chamber at 0.3 dyn/cm^2 for 30 s and at 0.4 dyn/cm^2 for 10 s. Perfusion was continued with HBSS medium containing 1 mM Ca(II) and 1 mM Mg(II) at 1 dyn/cm^2 for 10 s, and the shear was

doubled every 10 s up to 8 dyn/cm^2. Images of adherent cells were recorded through a 10× Nikon-Plan objective microscope on Hi-8 videotape at 30 frames per second for subsequent analysis. The middle 3 s of each shear was analyzed off-line using a computerized imaging system previously described (*10*). We tabulated the total number of adherent cells per field of view at each shear, the fraction of firmly adherent cells (defined as moving less than half of the cell diameter per 3 s interval), and the mean rolling velocity.

Experiments with streptavidin-coated polystyrene microspheres conjugated with N- or C-terminally biotinylated I domains were performed using the same experimental protocols as described for cells, except that the buffer was 2 mM Mg(II) in PBS (pH 7.4) and 1% BSA.

RESULTS

Construct Design. The integrin α_L I domain was fused either at its N-terminus to a 54-amino acid residue spacer and type II transmembrane domain or as previously described (*21*) at its C-terminus to a 54-amino acid residue spacer and a type I transmembrane domain (Figure 2A). Stable K562 transfectants were established that expressed the type II constructs slightly better than type I constructs with the wild-type α_L I domain (Figure 2B). As a control, transfectants were established that expressed the high-affinity K287C/K294C mutant α_L I domain comparably with either a type II or a type I TM domain (Figure 2B).

Comparison of Adhesion by Type I and Type II Anchored I Domains in Shear Flow. The adhesive behavior of K562 cells expressing type I and type II linked I domains was examined in parallel wall flow chambers with ICAM-1-Fcγ adsorbed to the lower wall. Cells were infused for 30 s at 0.3 dyn/cm^2, and then shear was incremented at 10 s intervals to 0.4, 1, 2, 4, and 8 dyn/cm^2. Type I transfectants accumulated predominantly at 0.3 and 0.4 dyn/cm^2, with additional accumulation at 1 dyn/cm^2 (Figure 3A). Only cells that moved more than half of the cell diameter per 3 s interval were counted as rolling in enumeration of rolling as opposed to firmly adherent cells (Figure 3A), but all cells were included in the calculation of rolling velocity (Figure 3C). Cells with type I TM-anchored I domains were shear-resistant, with most cells remaining adherent at 8 dyn/cm^2 (Figure 3A). The average rolling velocity increased from ~6 μm/s at 0.4 dyn/cm^2 to 22 μm/s at 8 dyn/cm^2 (Figure 3C). These results with type I TM-anchored I domain transfectants are consistent with previous results (*21*). Tethering and rolling were exclusively due to the I domain−ICAM-1 interaction as demonstrated by three lines of evidence. (1) No cells tethered and rolled on a mock (2% HSA) coated substrate. (2) No tethering and rolling were found when 1 mM Ca(II) and 1 mM Mg(II) were replaced with 5 mM EDTA. (3) Accumulation was inhibited by 97% by 10 μg/mL MHM24, an I domain blocking antibody.

Contrasting results were obtained with type II TM-anchored I domain transfectants. Type II transfectants accumulated less than 10% as efficiently as type I transfectants (Figure 3B). Furthermore, type II transfectants were far less shear-resistant, with no cells remaining adherent at 4 and 8 dyn/cm^2. Moreover, type II transfectants rolled 7−7.5-fold more rapidly than type I transfectants at 0.4 and 2 dyn/cm^2. The lower level of cell accumulation, the lower resistance to detachment, and the faster rolling velocity all show that the rolling adhesiveness of type II transfectants is markedly weaker than that of type I transfectants. This contrasts with the 1.3-fold higher level of I domain expression by the type II transfectants (Figure 2B). All other type II transfectant clones that were tested expressed smaller amounts of the I domain and were even more weakly adherent (data not shown). Accumulation of cells on the substrate was completely inhibited by 5 mM EDTA or 10 μg/mL MHM24 antibody.

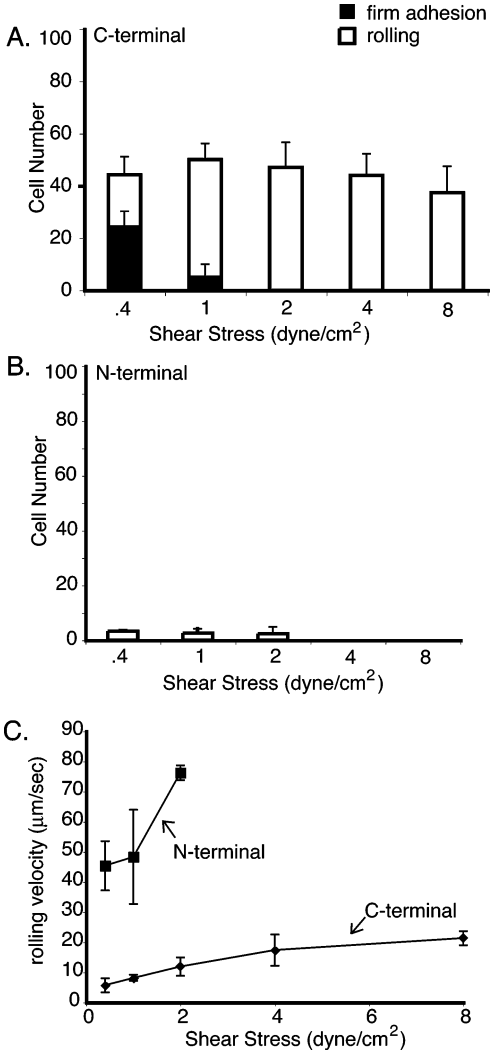

FIGURE 3: Adhesion in shear flow of K562 transfectants expressing wild-type I domains with type I or II TM domains. K562 transfectants expressing I domains with type I (C-terminal) or type II (N-terminal) TM domains were infused into the flow chamber in HBSS medium containing 1 mM Mg(II) and 1 mM Ca(II) with 10 μg/mL mouse IgG1 (control). Cells were allowed to accumulate at a wall shear stress of 0.3 dyn/cm^2 for 30 s in a parallel wall flow chamber with an ICAM-1-Fcγ substrate. The wall shear stress was increased to 0.4 dyn/cm^2 and incremented every 10 s. (A and B) Number of firmly adherent and rolling cells with type I (A) and type II (B) TM domains. (C) Average rolling velocity of all cells. Bars show the standard deviations of three experiments each with five replicates.

High-Affinity Mutant I Domain Type I and Type II Transfectants. The differences between the N- and C-terminally anchored I domains suggest that force, when applied along a pathway that favors a transition to an I domain conformation with higher affinity for ligand, can

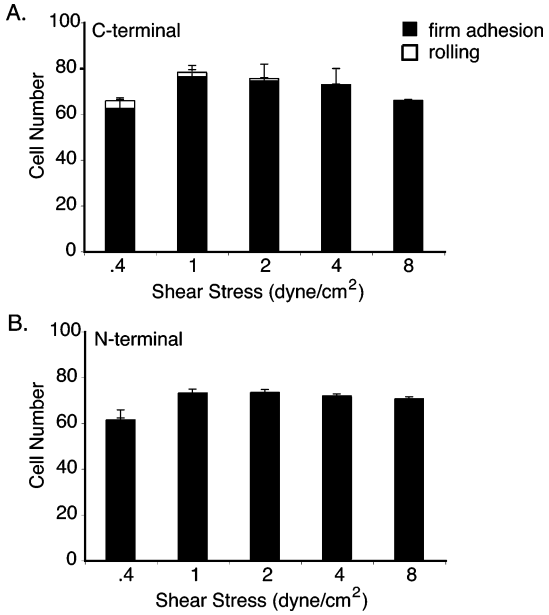

FIGURE 4: Adhesion in shear flow of K562 transfectants expressing high-affinity, mutant I domains with type I or II TM domains. K562 transfectants expressing high-affinity, K287C/K294C mutant I domains were infused exactly as described in the legend of Figure 3. (A and B) Number of firmly adherent and rolling cells with type I (A) and type II (B) TM domains. Bars show the standard deviations of three experiments each with five replicates.

stabilize rolling interactions. Our hypothesis predicts that differences between N- and C-terminally anchored constructs should not be found when a disulfide bridge is introduced between strand β6 and helix α7 that stabilizes the high-affinity conformation in the K287C/K294C mutant (*27*). The K287C/K294C mutant is already in the open conformation (*18*, *30*) that we hypothesize is favored by C-terminal force applied to the wild-type I domain; furthermore, the introduced disulfide should stabilize the I domain against any further conformational change when force is applied to the C-terminus. Indeed, high-affinity mutant type I and type II anchored I domain transfectants behaved identically in shear flow (Figure 4). The level of cell accumulation in shear flow and resistance to detachment at higher shear were slightly higher for the high-affinity mutant (Figure 4A) than for wild-type type I transfectants (Figure 3A) and were much higher for high-affinity type II transfectants (Figure 4B) than for wild-type type II transfectants (Figure 3B). Furthermore, essentially all of the cells were firmly adherent, even at the highest shear that was examined (Figure 4). Treatment with 5 mM EDTA or 10 μg/mL MHM24 antibody completely inhibited accumulation (data not shown).

Comparison of Adhesion by N- and C-Terminally Attached I Domains on Streptavidin-Coated Beads in Shear Flow. To exclude factors other than the intrinsic mechanochemistry of the I domain−ICAM-1 interaction as the source of the differential behavior, we studied streptavidin-coated polystyrene microspheres decorated with I domains specifically biotinylated near the N- or C-terminus. The biotin was enzymatically introduced on a specific lysine reside by biotin ligase (Figure 2C). We verified the display of equivalent amounts of N- and C-terminally attached I domains on microspheres (Figure 2D).

Similar numbers of beads with C- and N-terminally attached I domains accumulated on ICAM-1 substrates at

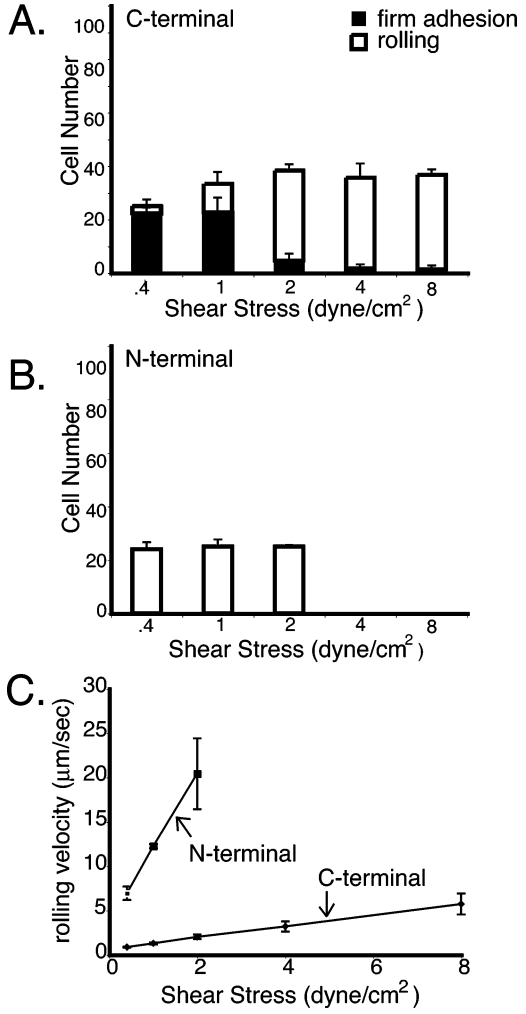

FIGURE 5: Adhesion in shear flow of microspheres decorated with N- or C-terminally linked I domains. Streptavidin-coated microspheres with I domains linked through C-terminal (A) or N-terminal (B) biotin tags were infused into a parallel wall flow chamber with an ICAM-1-Fcγ substrate in PBS containing 2 mM Mg(II) with 0.1% BSA and 10 μg/mL mouse IgG1 (control). Beads were allowed to accumulate at a wall shear stress of 0.3 dyn/cm^2 for 30 s. The wall shear stress was increased to 0.4 dyn/cm^2 and incremented every 10 s. (C) Average rolling velocity of all beads. Bars show the standard deviations of three experiments each with five replicates.

0.4 dyn/cm^2 (Figure 5A,B). Beads with C-terminally attached I domains accumulated further at 1 and 2 dyn/cm^2 (Figure 5A); in contrast, beads with N-terminally attached I domains did not accumulate at 1 and 2 dyn/cm^2 (Figure 5B). Furthermore, beads with C-terminally attached I domains were markedly more resistant to detachment. There was no detachment of beads with C-terminally attached I domains at a wall shear stress of up to 8 dyn/cm^2 (Figure 5A); by contrast, beads with N-terminally attached I domains were completely detached at 4 dyn/cm^2. The specificity of these interactions was demonstrated by the finding that replacing the Mg(II) with 5 mM EDTA or the addition of 10 μg/mL blocking MHM24 antibody specific for the α_L I domain eliminated all adhesion of the microsphere to the substrate (not shown).

The greater adhesive strength through C-terminally attached I domains was supported by measurements of rolling velocity. Using the operational definition of firm adhesion as a movement of less than half of a bead diameter per 3 s

period, C-terminally attached I domains mediated predominantly firm adhesion at 0.4 and 1 dyn/cm^2 and predominantly rolling adhesion at higher wall shear stresses (Figure 5A), whereas N-terminally attached I domains mediated only rolling adhesion (Figure 5B). Furthermore, C-terminally attached I domains mediated markedly slower rolling than N-terminally attached I domains (Figure 5C). The rolling velocity of beads with C-terminally attached I domains was 2.5-fold slower at 0.4 dyn/cm^2 and 11-fold slower at 2 dyn/cm^2 (Figure 5C). The rolling velocity increased linearly with shear with both types of beads. Our lab has provided the same C-terminally biotinylated I domain construct to another group, which obtained data in excellent quantitative agreement (*31*).

DISCUSSION

Here, we have tested the hypothesis that mechanical tension, exerted on a ligand-bound adhesion molecule that is resisting applied force, can couple with protein allostery to regulate adhesive interactions in shear flow. We explicitly tested this hypothesis by (1) expressing the integrin α_L I domain on transfectants anchored to a C-terminal type I TM domain or a N-terminal type II TM domain and (2) displaying the α_L I domain on cell-sized polystyrene beads attached through a C-terminal or N-terminal biotin tag. Compared to type II, N-terminally anchored I domains, the type I, C-terminally anchored I domains supported greater accumulation of transfectants in shear flow, greater resistance to detachment in shear flow, and slower rolling. By contrast, when the I domain was stabilized in the high-affinity conformation with a disulfide bond, the N- and C-terminally anchored I domain transfectants exhibited identical, strong adhesiveness. The results with wild-type I domains attached to beads through C- or N-terminal biotin tags resembled those with wild-type, cell-surface-anchored I domains. Compared to N-terminally attached I domains, the C-terminally attached I domains mediated accumulation at higher shear, were at least 4-fold more resistant to detachment by shear, and rolled with an ~10-fold slower velocity. The similar results with membrane-anchored and biotin-attached I domains allow us to rule out contributions to the differences observed between N- and C-terminal linkages (1) by the spacer sequences, which differ in the membrane-anchored and biotinylated constructs, and (2) specialized features of cells such as microvilli, deformability, and specific interactions with other proteins. The lack of differences between type I and II TM-anchored, high-affinity mutant I domain transfectants further supports these conclusions and demonstrates that differences between wild-type I domains are due to the effect of force on the C-terminal α helix.

Therefore, our results demonstrate mechanochemical regulation of adhesive interactions, whereby applied force, when appropriately linked to a pathway for conformational change, can enhance and stabilize adhesion. The results are explained schematically in Figure 1. When a cell or a bead bearing an I domain binds to ICAM-1 on a substrate in shear flow, the hydrodynamic force on the cell or bead is applied to the bound ICAM-1 and I domain molecules, their tethers (polypeptide spacer linkages) to the cell/bead and substrate, and the noncovalent receptor−ligand bond. The force is tensile and thus tends to lengthen the molecules and separate and hence weaken the receptor−ligand bond, resulting in a

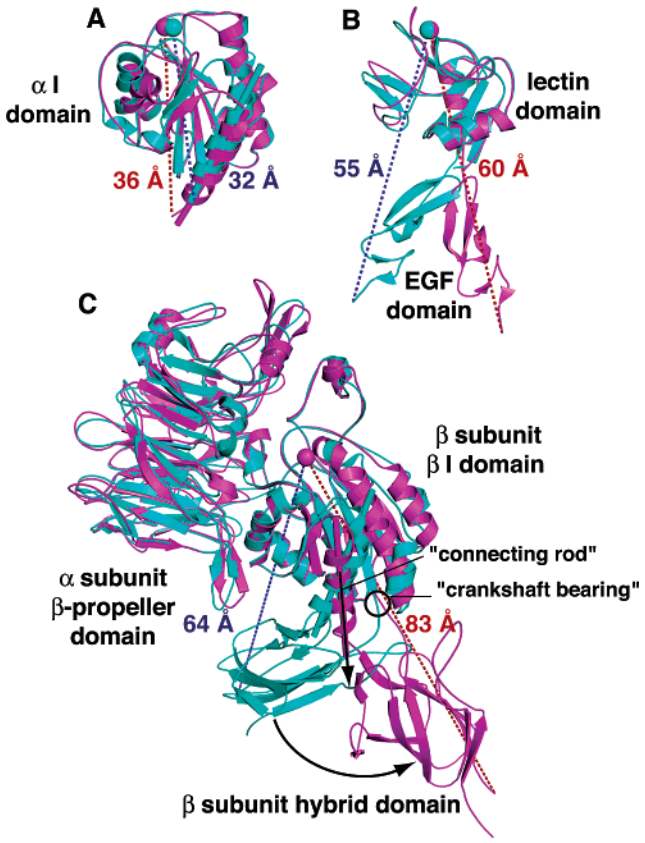

FIGURE 6: Mechanochemical design of adhesion molecules: (A) α_L I domain, (B) P-selectin, and (C) $\alpha_V\beta_3$ and $\alpha_{IIb}\beta_3$ headpieces. High-affinity, liganded (magenta) and low-affinity, unliganded (cyan) conformations are shown superimposed using backbone regions that move little between the two conformations. Dashed lines connect a Mg^{2+} (A and C) or Ca^{2+} (B) ion shown as a sphere in the center of the ligand-binding site to the most C-terminal residue shared between the pairs of structures, which in an intact adhesion molecule would connect to other domains that tether the adhesion molecule to the cell surface. The distances between the metal in the ligand binding site and this C-terminal residue, which tensile force would tend to increase, are shown. The dashed lines and distances are red for high-affinity, liganded conformations and blue for low-affinity, unliganded conformations. Solid cylinders emphasize the axes of the α7 helices of the α I domain (A) and β I domain (C) in each conformation. α_L I domain models (A) are from ref *24* and are based on refs *18* and *43*. P-Selectin lectin−EGF domain structures (B) are from ref *19*. $\alpha_V\beta_3$ (low-affinity, unliganded) and $\alpha_{IIb}\beta_3$ (high-affinity, liganded) headpiece structures (C) are from refs *15* and *16*.

k_{off} that increases exponentially with applied force (*32*). Since the MIDAS metal of the I domain lies in the center of the ICAM-1 binding site, the direction of the tensile force on the I domain can be modeled well by a line going through the MIDAS metal ion and the Cα atom of either the most C-terminal or N-terminal residue visualized in I domain crystal structures (Figure 6A). In I domain allostery, there is no movement of the N-terminus, which connects to strand β1, which is rigidly held in place as a central β strand in a β sheet with 321456 topology. Therefore, force applied to the N-terminus cannot stabilize one conformation relative to another. By contrast, C-terminal helix α7 is displaced axially by 7 Å toward its C-terminus during shape shifting from the closed, low-affinity to the high-affinity, open conformation (*17*) (Figure 6A). The vectors for C-terminal helix α7 displacement and tensile force applied to the C-terminus of the I domain are reasonably similar in

orientation (Figure 6A). Therefore, force is applied along a low-barrier trajectory that connects the two equilibrium conformational states and in the direction that stabilizes the high-affinity, open conformation. Thus, when force is applied through a C-terminal linkage, the increase in the extent of bond rupture by applied force can in part be offset by equilibration of the I domain to the high-affinity state by the applied force, with a resulting lower susceptibility to bond rupture by applied force. This mechanochemical effect of the applied force is clearly demonstrated here by the greater resistance to detachment, the lower rolling velocity, and the much more gradual increase in rolling velocity with an increase in shear seen with C-terminally as opposed to N-terminally attached receptors.

Previously, the ideas of "catch", "slip", and "catch−slip" bond behavior have been proposed and experimentally supported, and a change in bond lifetime in response to applied force has been modeled as resulting from a mechanochemical switch (*4*, *6*, *33*). However, the mechanical basis for a switch has been unclear, and it has been suggested that it might be in the ligand binding site (*4*). In our system, we have controlled for such effects, because the ligand binding site is identical in the N- and C-terminally tethered I domain constructs.

Our results demonstrate the crucial nature of the mechanical linkage to the I domain and provide one example of how a mechanochemical switch or rheostat can be designed: by applying the tensile force through a linkage in a way that favors conformational change to a higher-affinity state. In general, mechanochemical switches or rheostats will stabilize receptor−ligand bonds when the tensile force exerted on them favors a more extended, higher-affinity conformation. The biological relevance of this design principle is suggested below by a review of structural studies on integrins and selectins, the most important molecules for leukocyte adhesion in the vasculature; for both integrins and selectins, the more extended conformation has a higher affinity.

Selectins have been crystallized in a ligand-bound form in which the angle between the lectin and EGF domains is altered compared to molecules crystallized in the absence of ligand, resulting in a 5 Å increase in length between the Ca^{2+} at the ligand-binding site and the end of the EGF domain (*19*) (Figure 6B). Mutations designed to stabilize the more extended conformation increase the affinity for ligand (*34*), and the importance of selectin extension in supporting catch bond behavior has been hypothesized (*5*); however, tests of alternative force linkages as reported here have not been done and would be difficult because the N-terminal Trp residue is at the center of the lectin−EGF interface. Mutations in the linker between the lectin and pilin domains in an *Escherichia coli* fimbrae protein regulate shear-enhanced adhesion, and steered molecular dynamics and mutations support the hypothesis that linker extension is a key regulator of rolling behavior (*35*).

Both integrins that lack and contain α I domains exist in a bent, low-affinity conformation with the ligand binding site close to the cell membrane, and an extended, high-affinity conformation with the ligand binding site >100 Å farther from the cell surface as shown by crystal structures and electron microscopy (*15*, *16*, *36*, *37*). Thus far, atomic structures are available for isolated integrin α I domains (Figure 6A), but not for intact integrins containing α I domains. In the absence of an atomic structure revealing how integrin α I domains are inserted in the α subunit β propeller domain and are allosterically activated by the β subunit I domain (*38*, *39*), we can only speculate that applied force may also stabilize the high-affinity state of the α I domain in an intact integrin. However, atomic structures strongly support such a model for the β I domain.

The β I domain is present in all integrin β subunits and is structurally and functionally homologous to integrin α subunit I domains (*16*, *40*). The β I domain is also an inserted domain, with N- and C-terminal connections to the hybrid domain (Figure 6C). Structures are available for integrin ectodomain fragments crystallized with ligand in an open, high-affinity state and crystallized in the absence of ligand in a closed and bent, low-affinity state (*15*, *16*). Ligand is bound across the interface between the α subunit β propeller domain and the β subunit β I domain, and an acidic residue in the ligand coordinates to the β I domain MIDAS Mg^{2+} ion (Figure 6C). The β I domain undergoes shape shifting similar to that of the α I domain, with rearrangement of ligand-binding residues at the β I MIDAS coupled to an axial displacement by C-terminal helix α7. The piston and connecting rod-like movement of the connection of helix α7 to the hybrid domain and pivoting about the other, crankshaft bearing-like connection between the β I and hybrid domain cause the hybrid domain to swing 60° (*16*) (Figure 6C). Furthermore, the distance between the ligand binding site at the β I domain MIDAS metal ion and the most C-terminal residue in common between the two structures increases by 19 Å in the high-affinity state. Moreover, the vector for β I domain helix α7 displacement aligns well with the vector of applied force (Figure 6C). Integrins are anchored to the cell membrane by TM domains in both the α and β subunits; however, it is reasonable to expect that the β subunit has an important role in resisting applied force, because it is the subunit that is anchored to force-bearing cytoskeletal proteins, including talin for most integrin β subunits, and keratins for the β_4 subunit (*40*).

Individual adhesion receptor−ligand noncovalent bonds can bear forces in the range of 100 pN (*32*). Measurements of force-induced unfolding show that many domains, including domains 1 and 2 of ICAM-1 (J. Seog and T. Springer, unpublished results) (*41*), retain their native state in this range of force. Therefore, it is not unreasonable to use crystal structures to approximate the states accessible to force-loaded receptor−ligand complexes (Figure 6). The mechanochemical design of adhesion molecules described here will shift the conformational equilibrium toward the high-affinity, more extended conformation when force is applied to separate an adhesion molecule from a ligand to which it is bound (Figure 6). The applied tensile force will lower the free energy of the extended state relative to that of the basal state by approximately $F\Delta x$. Calculations for 10−100 pN tensile forces exerted on the selectin and integrin headpiece structures described above suggest that the extended conformation would be stabilized by the tensile force applied to the receptor by 0.5−25 kcal/mol. This would result in a substantial increase in the relative population of the extended, high-affinity conformation compared to the less extended, low-affinity conformation in the presence of tensile force. Favoring the high-affinity conformation when force is applied

(1) can give rise to catch bond behavior (*4*, *6*, *33*, *35*), (2) will dampen the increase in k_{off} by applied force (*8*), (3) will stabilize rolling adhesive interactions in shear flow and may explain the finding that only certain classes of receptor−ligand pairs can support rolling interactions (*10*), and (4) can account for both force resistance and mechanotransduction by integrins during cell adhesion and migration (*42*).

ACKNOWLEDGMENT

We thank Dr. G. Song for biotinylated protein and constructs with Bir A tags, Prof. L. W. Enquist for pAB35, Dr. T. Jensen for advice, Dr. Natasha Barteneva and Ken Ketman for cell sorting, and Ms. J. Martin for manuscript preparation.

REFERENCES

1. Chen, S., and Springer, T. A. (1999) An automatic braking system that stabilizes leukocyte rolling by an increase in selectin bond number with shear, *J. Cell Biol. 144*, 185−200.
2. Zhu, C., Long, M., Chesla, S. E., and Bongrand, P. (2002) Measuring receptor/ligand interaction at the single-bond level: Experimental and interpretative issues, *Ann. Biomed. Eng. 30*, 305−314.
3. Yago, T., Leppanen, A., Qiu, H., Marcus, W. D., Nollert, M. U., Zhu, C., Cummings, R. D., and McEver, R. P. (2002) Distinct molecular and cellular contributions to stabilizing selectin-mediated rolling under flow, *J. Cell Biol. 158*, 787−799.
4. Evans, E., Leung, A., Heinrich, V., and Zhu, C. (2004) Mechanical switching and coupling between two dissociation pathways in a P-selectin adhesion bond, *Proc. Natl. Acad. Sci. U.S.A. 101*, 11281−11286.
5. Konstantopoulos, K., Hanley, W. D., and Wirtz, D. (2003) Receptor-ligand binding: 'Catch' bonds finally caught, *Curr. Biol. 13*, R611−R613.
6. Marshall, B. T., Long, M., Piper, J. W., Yago, T., McEver, R. P., and Zhu, C. (2003) Direct observation of catch bonds involving cell-adhesion molecules, *Nature 423*, 190−193.
7. Shao, J. Y., Ting-Beall, H. P., and Hochmuth, R. M. (1998) Static and dynamic lengths of neutrophil microvilli, *Proc. Natl. Acad. Sci. U.S.A. 95*, 6797−6802.
8. Alon, R., Hammer, D. A., and Springer, T. A. (1995) Lifetime of the P-selectin: Carbohydrate bond and its response to tensile force in hydrodynamic flow, *Nature 374*, 539.
9. Springer, T. A. (1994) Traffic signals for lymphocyte recirculation and leukocyte emigration: The multi-step paradigm, *Cell 76*, 301−314.
10. Chen, S., Alon, R., Fuhlbrigge, R. C., and Springer, T. A. (1997) Rolling and transient tethering of leukocytes on antibodies reveal specializations of selectins, *Proc. Natl. Acad. Sci. U.S.A. 94*, 3172−3177.
11. van der Merwe, P. A., Barclay, A. N., Mason, D. W., Davies, E. A., Morgan, B. P., Tone, M., Krishnam, A. K. C., Ianelli, C., and Davis, S. J. (1994) Human cell-adhesion molecule CD2 binds CD58 (LFA-3) with a very low affinity and an extremely fast dissociation rate but does not bind CD48 or CD59, *Biochemistry 33*, 10149−10160.
12. de Chateau, M., Chen, S., Salas, A., and Springer, T. A. (2001) Kinetic and mechanical basis of rolling through an integrin and novel Ca^{2+}-dependent rolling and Mg^{2+}-dependent firm adhesion modalities for the $\alpha 4\beta 7$-MAdCAM-1 interaction, *Biochemistry 40*, 13972−13979.
13. Chan, P.-Y., Lawrence, M. B., Dustin, M. L., Ferguson, L. M., Golan, D. E., and Springer, T. A. (1991) Influence of receptor lateral mobility on adhesion strengthening between membranes containing LFA-3 and CD2, *J. Cell Biol. 115*, 245−255.
14. Chen, J. F., Takagi, J., Xie, C., Xiao, T., Luo, B.-H., and Springer, T. A. (2004) The relative influence of metal ion binding sites in the I-like domain and the interface with the hybrid domain on rolling and firm adhesion by integrin $\alpha 4\beta 7$, *J. Biol. Chem. 279*, 55556−55561.
15. Xiong, J.-P., Stehle, T., Diefenbach, B., Zhang, R., Dunker, R., Scott, D. L., Joachimiak, A., Goodman, S. L., and Arnaout, M. A. (2001) Crystal structure of the extracellular segment of integrin $\alpha V\beta 3$, *Science 294*, 339−345.
16. Xiao, T., Takagi, J., Wang, J.-h., Coller, B. S., and Springer, T. A. (2004) Structural basis for allostery in integrins and binding of ligand-mimetic therapeutics to the platelet receptor for fibrinogen, *Nature 432*, 59−67.
17. Lee, J.-O., Bankston, L. A., Arnaout, M. A., and Liddington, R. C. (1995) Two conformations of the integrin A-domain (I-domain): A pathway for activation? *Structure 3*, 1333−1340.
18. Shimaoka, M., Xiao, T., Liu, J.-H., Yang, Y., Dong, Y., Jun, C.-D., McCormack, A., Zhang, R., Joachimiak, A., Takagi, J., Wang, J.-h., and Springer, T. A. (2003) Structures of the α L I domain and its complex with ICAM-1 reveal a shape-shifting pathway for integrin regulation, *Cell 112*, 99−111.
19. Somers, W. S., Tang, J., Shaw, G. D., and Camphausen, R. T. (2000) Insights into the molecular basis of leukocyte tethering and rolling revealed by structures of P- and E-selectin bound to SLeX and PSGL-1, *Cell 103*, 467−479.
20. Knorr, R., and Dustin, M. L. (1997) The lymphocyte function-associated antigen 1 I domain is a transient binding module for intercellular adhesion molecule (ICAM)-1 and ICAM-1 in hydrodynamic flow, *J. Exp. Med. 186*, 719−730.
21. Salas, A., Shimaoka, M., Chen, S., Carman, C. V., and Springer, T. A. (2002) Transition from rolling to firm adhesion is regulated by the conformation of the I domain of the integrin LFA-1, *J. Biol. Chem. 277*, 50255−50262.
22. Huth, J. R., Olejniczak, E. T., Mendoza, R., Liang, H., Harris, E. A., Lupher, M. L., Jr., Wilson, A. E., Fesik, S. W., and Staunton, D. E. (2000) NMR and mutagenesis evidence for an I domain allosteric site that regulates lymphocyte function-associated antigen 1 ligand binding, *Proc. Natl. Acad. Sci. U.S.A. 97*, 5231−5236.
23. Shimaoka, M., Lu, C., Palframan, R., von Andrian, U. H., Takagi, J., and Springer, T. A. (2001) Reversibly locking a protein fold in an active conformation with a disulfide bond: Integrin α L I domains with high affinity and antagonist activity in vivo, *Proc. Natl. Acad. Sci. U.S.A. 98*, 6009−6014.
24. Jin, M., Andricioaei, I., and Springer, T. A. (2004) Conversion between three conformational states of integrin I domains with a C-terminal pull spring studied with molecular dynamics, *Structure 12*, 2137−2147.
25. Sanchez-Madrid, F., Krensky, A. M., Ware, C. F., Robbins, E., Strominger, J. L., Burakoff, S. J., and Springer, T. A. (1982) Three distinct antigens associated with human T lymphocyte-mediated cytolysis: LFA-1, LFA-2, and LFA-3, *Proc. Natl. Acad. Sci. U.S.A. 79*, 7489−7493.
26. Hildreth, J. E. K., Gotch, F. M., Hildreth, P. D. K., and McMichael, A. J. (1983) A human lymphocyte-associated antigen involved in cell-mediated lympholysis, *Eur. J. Immunol. 13*, 202−208.
27. Lu, C., Shimaoka, M., Ferzly, M., Oxvig, C., Takagi, J., and Springer, T. A. (2001) An isolated, surface-expressed I domain of the integrin $\alpha L\beta 2$ is sufficient for strong adhesive function when locked in the open conformation with a disulfide, *Proc. Natl. Acad. Sci. U.S.A. 98*, 2387−2392.
28. Brideau, A. D., del Rio, T., Wolffe, E. J., and Enquist, L. W. (1999) Intracellular trafficking and localization of the pseudorabies virus Us9 type II envelope protein to host and viral membranes, *J. Virol. 73*, 4372−4384.
29. Kalejta, R. F., Brideau, A. D., Banfield, B. W., and Beavis, A. J. (1999) An integral membrane green fluorescent protein marker, Us9-GFP, is quantitatively retained in cells during propidium iodide-based cell cycle analysis by flow cytometry, *Exp. Cell Res. 248*, 322−328.
30. Song, G., Lazar, G. A., Kortemme, T., Shimaoka, M., Desjarlais, J. R., Baker, D., and Springer, T. A. (2006) Rational design of ICAM-1 variants for antagonizing integrin LFA-1-dependent adhesion, *J. Biol. Chem. 281*, 5042−5049.
31. Eniola, A. O., Krasik, E. F., Smith, L. A., Song, G., and Hammer, D. A. (2005) I-domain of lymphocyte function-assocated antigen-1 mediates rolling of polystyrene particles, *Biophys. J. 89*, 3577−3588.
32. Chen, S., and Springer, T. A. (2001) Selectin receptor-ligand bonds: Formation limited by shear rate and dissociation governed by the Bell model, *Proc. Natl. Acad. Sci. U.S.A. 98*, 950−955.

33. Dembo, M., Torney, D. C., Saxman, K., and Hammer, D. (1988) The reaction-limited kinetics of membrane-to-surface adhesion and detachment, *Proc. R. Soc. London, Ser. B 234*, 55−83.
34. Phan, U. T., Waldron, T. T., and Springer, T. A. (2006) Remodeling of the lectin/EGF-like interface in P- and L-selectin increases adhesiveness and shear resistance under hydrodynamic force, *Nat. Immunol. 7*, 883−889.
35. Thomas, W. E., Trintchina, E., Forero, M., Vogel, V., and Sokurenko, E. V. (2002) Bacterial adhesion to target cells enhanced by shear force, *Cell 109*, 913−923.
36. Takagi, J., Petre, B. M., Walz, T., and Springer, T. A. (2002) Global conformational rearrangements in integrin extracellular domains in outside-in and inside-out signaling, *Cell 110*, 599−611.
37. Nishida, N., Xie, C., Shimaoka, M., Cheng, Y., Walz, T., and Springer, T. A. (2006) Activation of leukocyte β2 integrins by conversion from bent to extended conformations, *Immunity 25*, 583−594.
38. Yang, W., Shimaoka, M., Salas, A., Takagi, J., and Springer, T. A. (2004) Inter-subunit signal transmission in integrins by a receptor-like interaction with a pull spring, *Proc. Natl. Acad. Sci. U.S.A. 101*, 2906−2911.
39. Yang, W., Shimaoka, M., Chen, J. F., and Springer, T. A. (2004) Activation of integrin β subunit I-like domains by one-turn C-terminal α-helix deletions, *Proc. Natl. Acad. Sci. U.S.A. 101*, 2333−2338.
40. Springer, T. A., and Wang, J.-h. (2004) in *Cell Surface Receptors* (Garcia, K. C., Ed.) pp 29−63, Elsevier, San Diego.
41. Carrion-Vazquez, M., Oberhauser, A. F., Fisher, T. E., Marszalek, P. E., Li, H., and Fernandez, J. M. (2000) Mechanical design of proteins studied by single-molecule force spectroscopy and protein engineering, *Prog. Biophys. Mol. Biol. 74*, 63−91.
42. Chen, C. S., Tan, J., and Tien, J. (2004) Mechanotransduction at cell-matrix and cell-cell contacts, *Annu. Rev. Biomed. Eng. 6*, 275−302.
43. Qu, A., and Leahy, D. J. (1996) The role of the divalent cation in the structure of the I domain from the CD11a/CD18 integrin, *Structure 4*, 931−942.

BI061566O